Chapter 8

COMPTON THICK AGN: THE DARK SIDE OF THE X-RAY BACKGROUND

Andrea Comastri

INAF–Osservatorio Astronomico di Bologna
via Ranzani 1, I–40127, Bologna, Italy [*]

comastri@bo.astro.it

Abstract

The spectrum of the hard X-ray background records the history of accretion processes integrated over the cosmic time. Several pieces of observational and theoretical evidence indicate that a significant fraction of the energy density is obscured by large columns of gas and dust. The absorbing matter is often very thick, with column densities exceeding $N_H \simeq 1.5 \times 10^{24}$ cm^{-2}, the value corresponding to unity optical depth for Compton scattering. These sources are called "Compton thick" and appear to be very numerous, at least in the nearby universe. Although Compton thick Active Galactic Nuclei (AGN) are thought to provide an important contribution to the overall cosmic energy budget, their space density and cosmological evolution are poorly known. The properties of Compton thick AGN are reviewed here, with particular emphasis on their contributions to the extragalactic background light in the hard X-ray and infrared bands.

8.1   Introduction

Most of the active galactic nuclei (AGN) in the local universe are obscured in the X-ray band by large amounts of gas and dust, which prevent the observation of their nuclear emission up to energies that depend on the amount of intrinsic absorption. If the X-ray obscuring

matter has a column density which is equal to or larger than the inverse of the Thomson cross-section ($N_H \geq \sigma_T^{-1} \simeq 1.5 \times 10^{24}$ cm^{-2}), then the source is called, by definition, "Compton thick". The cross-sections for Compton scattering and photoelectric absorption have approximately the same value for energies of order 10 keV, which can be considered as the low energy threshold for probing the Compton thick absorption regime. Indeed, if the column density does not exceed a value of order 10^{25} cm^{-2}, then the nuclear radiation is visible above 10 keV, and the source is called mildly Compton thick. For higher column densities (heavily Compton thick), the entire high energy spectrum is downscattered by Compton recoil and hence depressed over the entire X-ray energy range. The presence of Compton thick matter may be inferred through indirect arguments, such as the presence of a strong iron Kα line complex at $6.4 - 7$ keV and the characteristic reflection spectrum.

The study of Compton thick sources is relevant for several reasons: (1) there is observational evidence that suggests that a large fraction of AGN in the local universe are obscured by Compton thick gas (Maiolino et al. 1998; Risaliti, Maiolino, & Salvati 1999a; Matt et al. 2000); (2) a sizable population of mildly Compton thick sources is postulated in all the AGN synthesis models for the X-ray background (XRB) in order to match the intensity peak of the XRB spectrum at about 30 keV. The absorbed luminosity eventually will be reemitted in the far-infrared (far-IR), making Compton thick sources potential contributors to the long wavelength background. Finally, accretion in the Compton thick AGN may contribute to the local black hole mass density.

Unfortunately, the most efficient energy range to search for mildly Compton thick sources is just above the highest energy accessible to the past and present generation of satellites with imaging capabilities for faint limiting fluxes. As a consequence, the search for Compton thick sources has been limited, so far, to the relatively bright fluxes accessible to the high energy detectors onboard *BeppoSAX* and *RXTE*.

In this chapter, we review the evidence for obscured AGN, with a special emphasis on the evidence for Compton thick sources. We then examine in some detail the contributions of Compton thick sources to the XRB.

8.2 Absorption Distribution in the Local Universe

According to the so-called AGN unified model (Antonucci 1993), Seyfert II galaxies are powered by the same engine (a supermassive black hole plus an accretion disk) as Seyfert I galaxies, but they are viewed through

a geometrically and optically thick structure of gas and dust with an axisymmetric geometry (known as the "torus") that absorbs the nuclear radiation at ultraviolet (UV)/optical and soft X-ray energies. The distinction between type I and type II galaxies originally was conceived to classify objects characterized by different properties at UV and optical wavelengths. Both broad and narrow lines are visible over a strong blue UV-optical continuum in type 1 galaxies, while only narrow lines are observed in type 2 galaxies.

In the simplest version of the unified models, X-ray obscured sources are expected to be uniquely associated with optical type II sources. The increasing evidence of a mismatch between optical and X-ray classification (which will be discussed in the following sections) suggests that the terms type I and type II should be treated with caution and should always be referenced to a specific band. Following Matt (2002), in this review, I will use the original meaning of type II and type I, which is based on optical spectroscopy.

The amount of obscuring material can be measured best in the hard $(2 - 10$ keV) X-ray band, which is transparent up to column densities of order 10^{24} cm^{-2} (i.e., Compton thin); hence, hard X-ray surveys are a powerful method to obtain large, unbiased samples of obscured AGN. Since the first observations, it has been realized that the large majority of Seyfert II galaxies contain obscured AGN, which are fairly strong X-ray sources with $2 - 10$ keV luminosities up to 10^{44} ergs s^{-1}.

The relative fraction of sources with a given column density depends on the survey sensitivity at high energies and on the amount of obscuring gas. The larger the column density, and/or the lower the sensitivity, the stronger will be the observational bias against the discovery and identification of obscured AGN. Such a bias is maximal for (mildly) Compton thick sources due to the rapidly decreasing effective area at high energies of the most sensitive space observatories (the *Chandra* and *XMM-Newton X-ray Observatories*). Thus, we cannot measure the photoelectric cutoff and the corresponding N_H value. Moreover, even observations in the hard X-ray domain above 10 keV do not allow the sampling of column densities of order 10^{25} cm^{-2} or larger because the entire high energy spectrum is down-scattered by Compton recoil to lower energies, where it is readily absorbed (see Fig. 8.1). The high energy spectra of obscured AGN are often much more complex than a single absorbed power law. Additional components (i.e., thermal emission from a starbursting region and/or nuclear flux scattered into the line of sight) are common in the X-ray spectra below 10 keV of several nearby Compton thick galaxies (Matt et al. 1997; Vignati et al. 1999). The photoelectric cut-off (if any) does not provide a measure of the "true" nuclear absorption anymore.
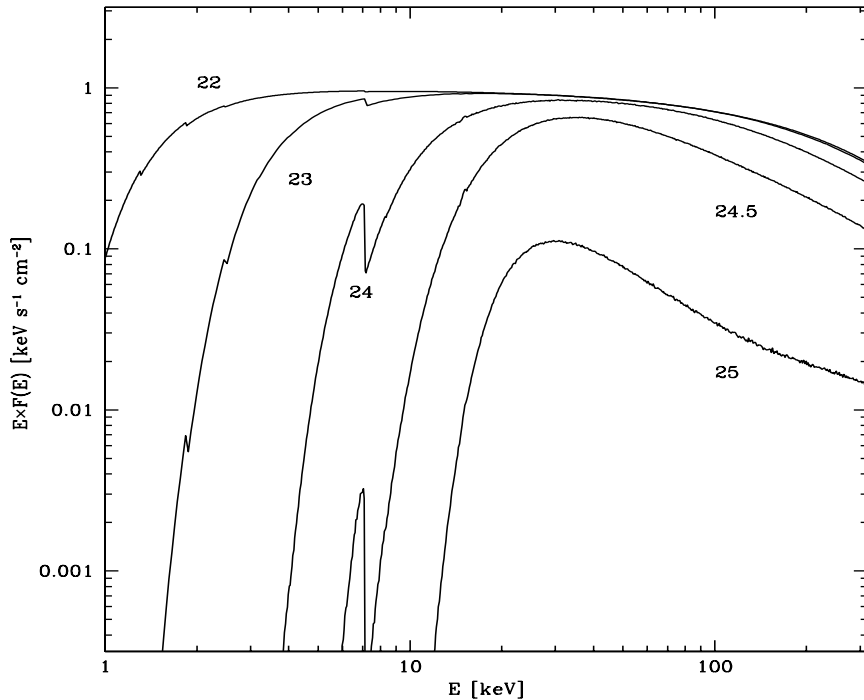
Figure 8.1. Effects of photoelectric absorption and Compton down-scattering on the typical AGN X-ray spectrum (a power law with photon index $\Gamma = 2$, plus an exponential cut-off at 300 keV). Labels correspond to the logarithm of the column density.

A powerful diagnostic of the presence of obscuring, possibly Compton thick, matter is provided by the intensity of the iron line, which is expected to be produced both by transmission through (Leahy & Creighton 1993) and/or reflection by absorbing gas (Ghisellini, Haardt, & Matt 1994; Matt, Brandt, & Fabian 1996).

As far as the transmitted continuum is concerned, the line equivalent width (EW) increases with the column density (since it is measured against an absorbed continuum) and reaches values of order 1 keV for $N_H \sim 10^{24}$ cm^{-2}. Larger values for the EW (up to several keV) can be obtained for high inclination angles and small torus opening angles (Levenson et al. 2002).

The signature of Compton thick matter is also imprinted on the "reflected" light, the so-called "Compton reflection" continuum characterized by a broad bump peaking around $20 - 30$ keV, which rapidly decreases at both low and high energies due to absorption and Compton down-scattering, respectively. In the $2 - 10$ keV range, it is well ap-

proximated by a flat power law. The iron line EW with respect to the reflected continuum is always greater than 1 keV (George & Fabian 1991; Matt, Perola, & Piro 1991).
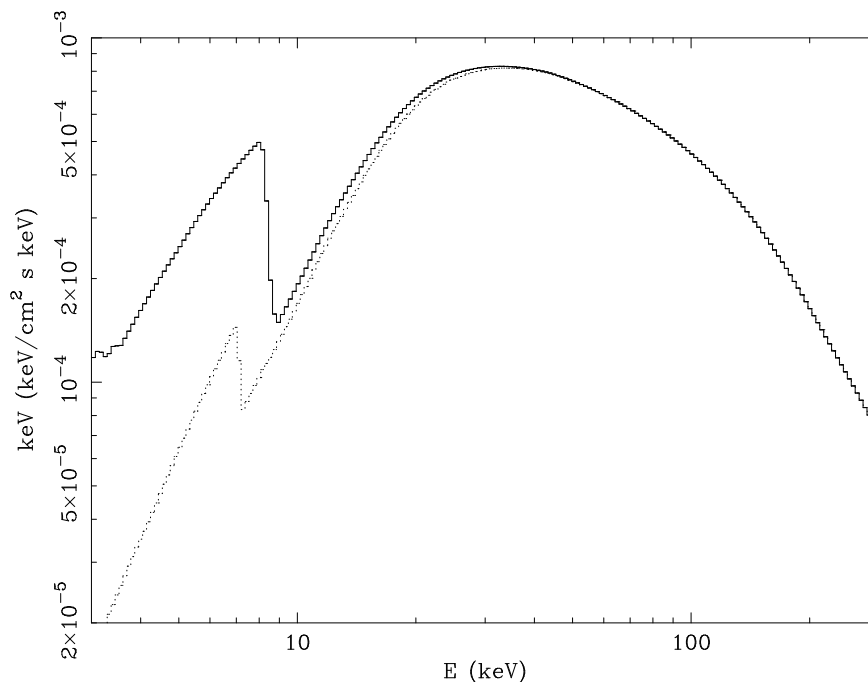

Figure 8.2. Spectrum reflected by Compton thick gas. Dotted curve corresponds to neutral gas; solid curve corresponds to highly ionized material.

The shape of the reflection spectrum (reported in Fig. 8.2 for two specific examples) is also a function of the column density, the ionization status, and the metallicity of the reflecting matter (Matt 2002). Its intensity depends upon the solid angle subtended by the reflector at the primary illuminating source. The gas is more reflective if highly ionized, and the effect is significant at energies below $7 - 8$ keV.

Despite the presence of other spectral components, such as thermal emission from a hot plasma with a range of temperatures, and/or scattered nuclear light that may dilute the typical reflection spectrum, the signature of Compton thick matter (i.e., a strong iron Kα line) has been unambiguously revealed already with the *ASCA* satellite in several nearby bright objects (i.e., the Circinus galaxy, Matt et al. 1996; NGC 6240, Iwasawa & Comastri 1998).

Within the framework of the unified scheme, a further method for evaluating N_H has been proposed by Bassani et al. (1999). For a heterogeneous but sizable sample of Seyfert II galaxies, they found that the

ratio between the $2 - 10$ keV and the dereddened [OIII] flux (assumed to be an isotropic indicator of the intrinsic luminosity) is anti-correlated with the absorption column density and the EW of the iron line. Such a relationship could be used to select candidate Compton thick AGN, especially among those weak sources for which X-ray spectroscopy is not feasible. In this regard, it is interesting to note that the Seyfert II galaxy NGC 5135, characterized by a very low value of $F_X/F_{\text{[OIII]}}$ and suspected to be Compton thick, is now unambiguously classified as such, thanks to the detection of a strong iron line in the *Chandra* spectrum (Levenson et al. 2004).

A significant step forward in the study of highly obscured AGN has been made with the Phoswich Detector System (PDS) instrument on-board *BeppoSAX*, which made accessible, for the first time, the $10 - 100$ keV energy range down to limiting fluxes of order 10^{-11} ergs cm^{-2} s^{-1}. Deep exposures of a sample of seven nearby, bright objects selected by the presence of the characteristic features described above allowed the intrinsic nuclear spectrum above 10 keV to be unambiguously uncovered in 5 out of the 7 sources, and column densities in the range $1-5 \times 10^{24}$ cm^{-2} to be measured (see Matt et al. 2000 for a review).

The issue of how common Compton thick sources are and whether they constitute a sizable fraction of the Seyfert population has been addressed by Maiolino et al. (1998) and Risaliti et al. (1999a). Starting from a sample of local Seyfert II galaxies selected on the basis of their [OIII] flux, and using *ASCA* and *BeppoSAX* observations, they concluded that about half of the objects are obscured by column densities $N_H > 10^{24}$ cm^{-2}. Given the lack of complete spectral coverage at energies > 10 keV with *BeppoSAX*, the relative fraction of heavily ($N_H > 10^{25}$ cm^{-2}) and mildly ($10^{24} < N_H < 10^{25}$ cm^{-2}) Compton thick sources remained poorly constrained.

Several independent arguments suggest that the space density of Compton thick sources, at least in the local universe, could be high. For example, two out of the three nearest AGN within 4 Mpc are mildly Compton thick (NGC 4945 and Circinus; the third source, Cen A, is also obscured with $N_H \simeq 10^{23}$ cm^{-2}). A simple estimate obtained by integrating the AGN luminosity function indicates that heavily obscured AGN could outnumber unobscured AGN by about one order of magnitude (see Matt et al. 2000 for a detailed discussion).

The optical appearance of Compton thick AGN may also contribute to raising the estimate of their space density. Indeed, two bright objects (NGC 4945 and NGC 6240) are classified as LINERs (Low Ionization Nuclear Emission Regions) on the basis of their optical spectra and, as a consequence, have not been included in the sample of Risaliti et

al. (1999a). The detection of Compton thick matter in objects with broad optical emission lines (type I; Guainazzi, Stanghellini, & Grandi 2003; Iwasawa, Maloney, & Fabian 2002) highlights the uncertainties associated with the estimates of the occurrence of Compton thick absorption. More examples of AGN that do not show any Seyfert signatures in the optical band have been reported recently by Maiolino et al. (2003): *Chandra* observations of a small sample of this class of optically "elusive" nuclei indicate that most of them are obscured by column densities exceeding 10^{24} cm^{-2}. Their space density is comparable or even higher than that of optically selected Seyfert nuclei, implying that the ratio between obscured and unobscured AGN is larger than previously estimated.

It is also worth mentioning that high amplitude variability may play an important role in the source classification. Several convincing examples have been discussed by Matt, Guainazzi, & Maiolino (2003) where a transition from a reflection dominated spectrum to Compton thin and vice versa has been detected on timescales of order a few years. The most likely explanation entails strong variability of the continuum nuclear source and a Compton thick reflector on the parsec scale, possibly associated with the absorbing torus. If the nuclear source is switched off, only the reflected light is detected. Conversely, if the primary continuum source is switched on, the reflected component is not dominant anymore. Although such an effect should not change, on average, the relative ratio between Compton thick and Compton thin absorbers, it adds further uncertainties in the estimates of the absorption distribution and may also explain the mismatches between optical and X-ray classifications if the observations at different wavelengths are not simultaneous.

On the basis of what has been discussed above, it is concluded that Compton thick absorption is quite common among Seyfert galaxies in the local universe. Several independent lines of evidence suggest that mildly and heavily Compton thick sources are likely to dominate the absorption distribution observed in nearby AGN. The covering factor of the Compton thick gas must therefore be large.

A compilation of column densities in the Compton thick regime collected from the literature is reported in Table 8.1 for objects observed above 10 keV with *BeppoSAX*. The Compton thick nature of sources observed below 10 keV, inferred from the presence of a strong iron line, is reported in Table 8.2. Due to the lack of coverage above 10 keV, only a conservative lower limit could be placed on the intrinsic column density.

The majority of the sources are low redshift ($z < 0.05$), relatively low luminosity ($L_X < 10^{43}$ ergs s^{-1}) Seyfert II galaxies. Several interesting exceptions, however, do exist and will be discussed in the next section.

Table 8.1. Compton thick galaxies observed by *BeppoSAX*

Source Name	Opt. Class.	z	N_{H} $(10^{24}\ \mathrm{cm}^{-2})$	$L_{2-10\ \mathrm{keV}}$ $(10^{44}\ \mathrm{ergs\ s}^{-1})$	Ref.
NGC 1068	Sy2	0.0038	≥ 10	> 1	(1,2)
Circinus	Sy2	0.0014	4.3	0.01	(2,3)
NGC 6240	LINER	0.0243	2.2	1.2	(4)
Mrk 3	Sy2	0.0134	1.1	0.9	(5,6)
NGC 7674	Sy2	0.0289	≥ 10	2	(7)
NGC 4945	LINER	0.0019	2.2^{a}	0.03	(8)
Tol 0109−383	$\mathrm{Sy2}^{b}$	0.0116	2.0	0.2	(9)
IRAS 09104+4109	$\mathrm{QSO2}^{c}$	0.442	$\geq 5^{d}$	80	(10)
NGC 3690	HII	0.011	2.5	0.2	(11)
NGC 3281	Sy2	0.0115	2.0	0.23	(12)
M 51	LINER/Sy2	0.0015	5.6	0.0011	(13)
NGC 3079	LINER/Sy2	0.0038	10	0.01–0.1	(14)
S5 1946+708	RadioGal	0.101	> 2.8	> 36	(15)
PKS 1934−63	RadioGal	0.182	>1	> 1.9	(15)
IRAS 20210+1121	Sy2	0.0564	> 10	0.022	(16)
IC 3639	Sy2	0.0110	> 10	0.09	(17)
NGC 1386	Sy2	0.0029	> 1	0.04	(18)
NGC 2273	Sy2	0.0062	> 10	0.08	(18)
NGC 3393	Sy2	0.0125	> 10	0.1	(18)
NGC 4939	Sy2	0.0104	> 10	0.3	(18)
NGC 5643	Sy2	0.0039	> 10	0.045	(18)
MCG−05−18−002	Sy2	0.0056	> 10	0.05	(18)
IRAS 11058−1131	Sy2	0.0548	> 10	2.6	(19)
Mrk 266	Sy2	0.0279	> 10	0.9	(19)
IRAS 14454−4343	Sy2	0.0386	> 10	0.7	(19)

References — (1) Matt et al. 1997; (2) Guainazzi et al. 1999; (3) Matt et al. 1999; (4) Vignati et al. 1999; (5) Cappi et al. 1999; (6) Matt et al. 2000; (7) Malaguti et al. 1998; (8) Guainazzi et al. 2000; (9) Iwasawa et al. 2001; (10) Franceschini et al. 2000; (11) Della Ceca et al. 2002; (12) Vignali & Comastri 2002; (13) Fukazawa et al. 2001; (14) Iyomoto et al. 2001; (15) Risaliti, Woltjer, & Salvati 2003; (16) Ueno et al. 1998; (17) Risaliti et al. 1999b; (18) Maiolino et al. 1998; (19) Risaliti et al. 2000.

Table notes — [a]In Schurch, Roberts, & Warwick (2002), ~ 4 using *Chandra* plus *XMM-Newton* observations. [b]See also Murayama, Taniguchi, & Iwasawa (1998) for a different optical classification. [c]Hyperluminous infrared galaxy with strong narrow emission lines (Kleinmann et al. 1988). [d]Iwasawa et al. (2001) find 3.3 using a *Chandra* observation.

The $2-10$ keV luminosities are corrected for intrinsic absorption assuming the best fit spectral parameters reported in the literature. It is important to point out that for high column densities, the intrinsic luminosity is strongly dependent upon the precise value of absorption. For this reason, the luminosities should be considered only indicative and subject to substantial uncertainties. This is even more true for those

sources for which only a lower limit for the intrinsic column density is available. The $2-10$ keV luminosity has been estimated assuming that 1% of the intrinsic luminosity is actually observed below 10 keV, due to scattering and or reflection. This assumption, though reasonable and supported by some observational evidence (Turner et al. 1997), is not always the rule for Compton thick sources. Although all efforts have been made to make the list as complete as possible, some objects could have been missed. Moreover, the sample is by no means complete and should not be used for statistical investigations.

Table 8.2. Compton thick galaxies observed at $E < 10$ keV

Source Name	Opt. Class.	z	N_{H} $(10^{24} \mathrm{\ cm}^{-2})$	$L_{2-10 \mathrm{\ keV}}$ $(10^{44} \mathrm{\ ergs\ s}^{-1})$	Ref.
Mrk 1066	Sy2	0.0121	> 1	0.07	(20)
NGC 5005	Sy2/LINER	0.0032	> 1	0.0064	(20)
NGC 5347	Sy2	0.0078	> 1	0.05	(20)
IC 5135	Sy2	0.0161	> 1	0.3	(20)
NGC 5135	Sy2	0.0137	> 1	0.075	(21)
NGC 1667	Sy2	0.0152	> 1	0.01	(21)
Mrk 1210	Sy2	0.0135	> 1	0.8	(21)
Mrk 477	Sy2/NLSy1	0.0378	> 1	5	(21)
ESO 138−G1	Sy2	0.0091	> 1.5	0.33	(22)
OQ +208	RL QSO	0.077	> 1	≥1.4	(23)
NGC 6552	Sy2	0.0262	> 1	1.2	(24)
IC 2560[e]	Sy2	0.0097	> 1[f]	0.03	(25)
NGC 2623	LINER	0.0185	> 1	0.1	(26)
NGC 4418	LINER	0.0073	> 1	0.0016	(26)
UGC 5101	LINER	0.0394	> 1	0.2	(27)
NGC 4968[h]	Sy2	0.0099	> 1 ?	0.15	(28)
IRAS 19254−7245	HII	0.062	≥ 1	10	(29)
IRAS F12514+1027	QSO/Sy2	0.30	> 1.5	> 1.8	(30)

References — (20) Risaliti et al. 1999a; (21) Bassani et al. 1999; (22) Collinge & Brandt 2000; (23) Guainazzi et al. 2003; (24) Risaliti et al. 2000; (25) Iwasawa et al. 2002; (26) Maiolino et al. (2003); (27) Ptak et al. 2003. (28) Guainazzi et al. 2002; (29) Braito et al. 2003; (30) Wilman et al. 2003.

Table notes — [e] See also Risaliti et al. (1999a) for the *BeppoSAX* observation. [f] From the iron Kα line EW, find > 3. [h] See also Bassani et al. (1999; candidate Compton thick galaxy).

8.3 Compton Thick AGN and the XRB

The amount of obscuring gas in Seyfert galaxies and quasars, and the distribution of column density as a function of redshift and luminosity, are key ingredients in the X-ray background synthesis models. First predicted by Setti & Woltjer (1989) and elaborated on with an increasing degree of detail by several authors (Madau, Ghisellini, & Fabian 1994; Comastri et al. 1995; Gilli, Salvati, & Hasinger 2001), the XRB spectral energy density is due to the integrated contribution of highly obscured AGN.

Although a detailed description of population synthesis models for the XRB is beyond the purposes of the present chapter, it might be useful to summarize briefly the main features (see Comastri 2001 for more details). The basic recipe to "cook" the so-called baseline model is a rather straightforward three-step approach. (1) Assume as a template for unobscured (type I) sources the average spectrum of nearby Seyfert I galaxies above 2 keV, parameterized as a steep ($\Gamma = 1.9$) power law plus a reflection component from a face-on disk and a high energy cutoff at about 300 keV. (2) Add to the template a distribution of column densities with $\log N_H$ in the range $21 - 25$ cm^{-2} to model the obscured (type II) AGN population. (3) Fold both the type I and type II spectra with an evolving X-ray luminosity function (XLF) with best fit parameters determined from soft X-ray surveys and appropriate for unobscured AGN.

The column density distribution is varied in both shape and normalization until a good fit to the XRB spectrum, source counts in different energy bands, and redshift distributions at different limiting fluxes is obtained. While at first glance it seems that the only parameters that are free to vary are those related to the absorption distribution, it must be stressed that the best fit values adopted for the evolving XLF and spectral templates are also subject to non-negligible uncertainties that are not taken into account in the baseline model. In particular, the assumptions concerning the XLF evolution of the obscured population, though in line with a strict version of the AGN unified scheme, do not have any observational support. It is thus remarkable that a such a model was able to reproduce all of the observational constraints available in the pre-*Chandra/XMM-Newton* era. It is also worth remarking that the baseline model (as well as all of the models proposed so far) is purely X-ray based: the optical appearance of an obscured source may not necessarily be that of an optically selected type II AGN.

The integrated contributions of unobscured and obscured AGN, the latter split into Compton thin and Compton thick AGN, are reported
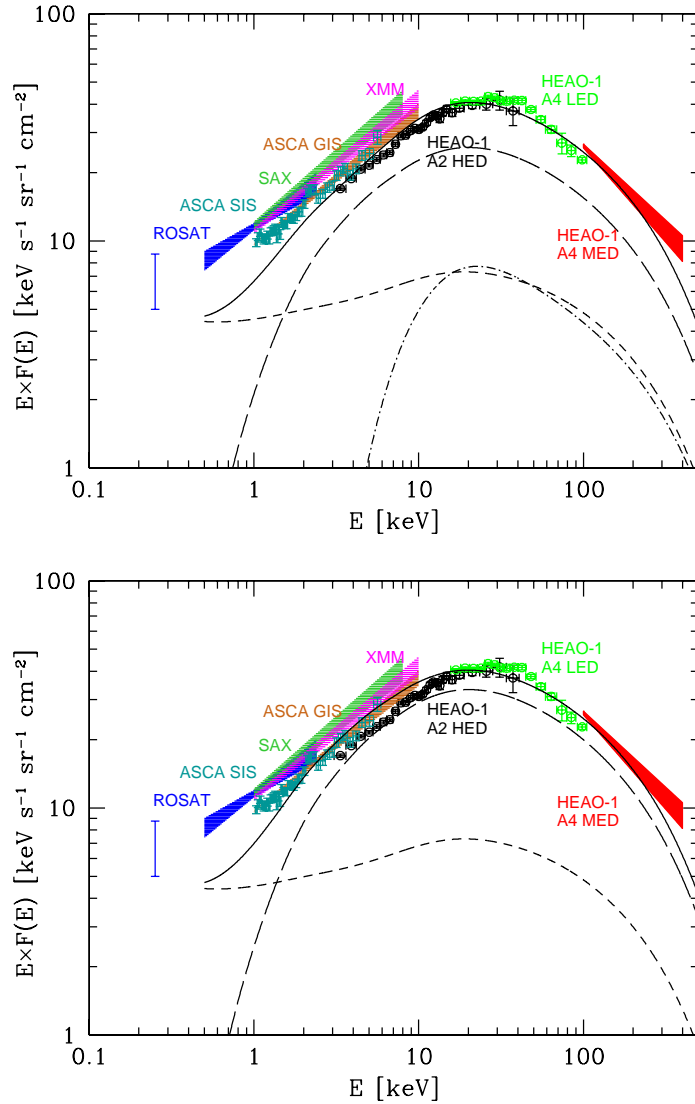
Figure 8.3. *(Top panel)* AGN contribution *(solid line)* to the XRB spectral energy density, as measured by different instruments *(labeled)*. Contributions of unobscured *(dashed line)*, Compton thin *(long-dashed line)*, and Compton thick *(dot-dashed line)* AGN are also shown. Labels refer to XRB measurements obtained by different satellites. *(Bottom panel)* Same as above, but without Compton thick AGN.

in Figure 8.3 (adapted from Comastri et al. 2001). Even though such a model is not able to reproduce some of the recent observational constraints emerging from deep *Chandra* and *XMM-Newton* surveys—in

particular, the observed redshift distribution—it can be considered representative of most of the population synthesis models, at least regarding the contribution of Compton thick sources to the broadband XRB spectrum (see, for example, Fig. 5 in Wilman & Fabian 1999). Indeed, in the synthesis model of Ueda et al. (2003), where a more satisfactory description of the recent observational constraints is obtained, the integrated contribution of mildly Compton thick sources is very similar to that shown in Figure 8.3.

Not surprisingly, mildly Compton thick sources provide a non-negligible contribution only around the peak energy of the XRB spectrum, while it is clear that most of the energy density is accounted for by obscured, Compton thin AGN.

Given that the overall shapes of Compton thin and Compton thick AGN, once convolved with the evolving XLF, are very similar, it seems reasonable to argue that the XRB spectrum could be equally well fitted without invoking Compton thick absorption. Indeed, this appears to be the case: an acceptable fit to the XRB spectrum can be obtained just by rescaling the absorption distribution of Compton thin AGN (see Fig. 8.3).

However, the relative fraction of absorbed ($N_H > 10^{22}$ cm^{-2}) sources as a function of the $2-10$ keV flux is significantly overestimated over the entire range of fluxes (solid line in Fig. 8.4). While the model that includes Compton thick absorption does fit the observations at both very bright and faint fluxes better (dashed line in Fig. 8.4), the absorption distribution measured by shallow, large-area *ASCA* and *XMM-Newton* surveys is not well matched. Such a discrepancy, together with the redshift distribution of obscured AGN, is challenging the standard model for the XRB, at least in its simplest form, calling for some revision of the basic assumptions. A detailed comparison of XRB modeling versus observations is beyond the purposes of this chapter. The bottom line of the exercise described above is that Compton thick absorption cannot be neglected in building up a synthesis model for the XRB.

On the other hand, it is also possible to fit the XRB spectrum with a model where the contribution of heavily Compton thick AGN is dominant. This possibility has been put forward by Fabian et al. (1990), who showed that the $10-300$ keV background intensity can be accounted for by the integrated contribution of luminous sources at $\langle z \rangle \sim 1.5$ with the characteristic Compton "reflection" spectrum (see Fig. 8.2). The most interesting feature of this model is the natural explanation of the XRB 30 keV peak in terms of a physical process that is basically driven by the Thomson cross-section, σ_T. The integrated spectrum of Compton reflection dominated sources is, however, too hard and does not fit the
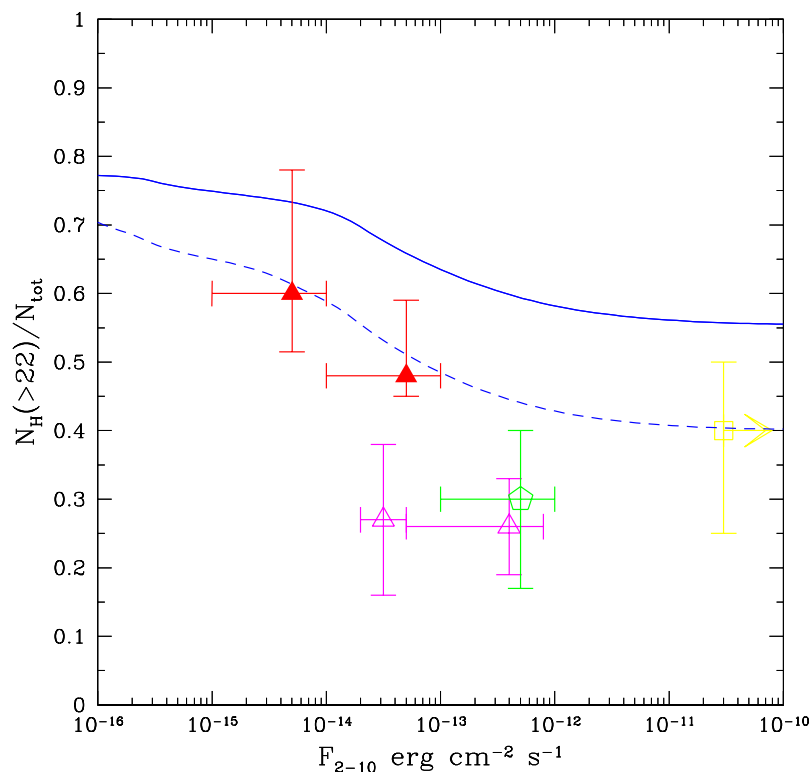
Figure 8.4. Expected fraction of sources with absorption column densities larger than 10^{22} cm^{-2} vs. $2-10$ keV flux for a model without *(solid line)* and with *(dashed line)* Compton thick sources. Points and associated error bars correspond to the observed fraction of absorbed sources in different X-ray surveys: open square at bright X-ray fluxes is from the *HEAO1-A2* AGN sample of Piccinotti et al. (1982), open hexagon is from the *ASCA* Large Sky Survey (Akiyama et al. 2000), open triangles are from *XMM-Newton* observations (Piconcelli et al. 2002), and filled triangles are from *Chandra* observations (Brusa 2004).

data below 10 keV; moreover, the source counts in the $0.3-3.5$ keV band (the only available at that time) were strongly underestimated (Comastri 1991; Terasawa 1991).

Although such an extreme hypothesis is ruled out by the data, it has been pointed out that the 30 keV peak can be better reproduced including a "reflection" component (Gilli et al. 2001; Ueda et al. 2003) with a covering factor of about 2π (Fig. 8.5) in the spectral templates of both unobscured and obscured AGN.

On the basis of these considerations, it is safe to conclude that absorption and reflection from Compton thick matter need to be included
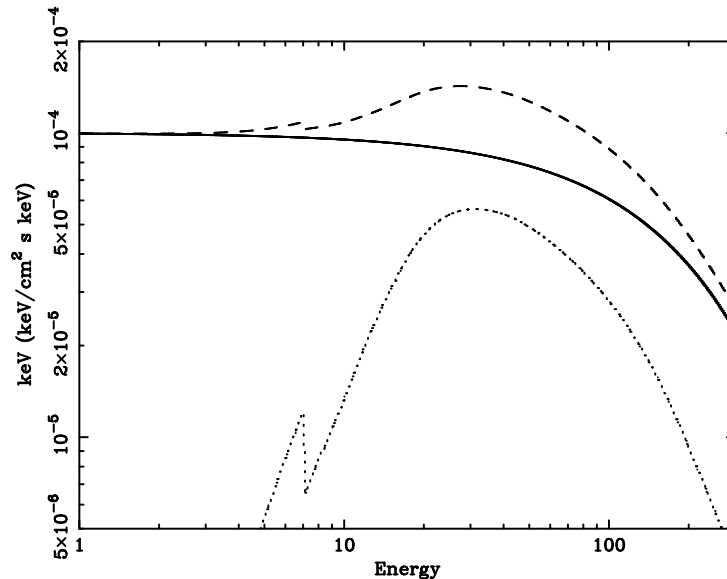
Figure 8.5. Long dashed curve is the X-ray spectrum after reflection from cold thick matter subtending 2π sr at the illuminating continuum source—a power law with $\Gamma = 2$ plus an exponential cut-off at 300 keV *(solid curve)*. Dotted curve shows the reflected component.

in the high energy spectra of the sources responsible for the hard XRB. While there is compelling evidence (see § 8.2) for a numerous population of Compton thick AGN in the nearby universe, their space density at cosmological distances is still basically unknown.

8.4 Distant Obscured AGN

Thanks to deep and medium-deep *Chandra* and *XMM-Newton* surveys (Giacconi et al. 2002; Alexander et al. 2003; Hasinger et al. 2001), it is now possible to search for obscured AGN at much larger distances. The determination of the intrinsic column density requires that the source redshift be known. Extensive campaigns of optical identifications have started to produce sizable samples of spectroscopically identified sources (Barger et al. 2002, 2003; Mainieri et al. 2002; Szokoly et al. 2004).

Most of the hard X-ray selected sources are obscured by column densities $10^{21} < N_H < 10^{23}$ cm^{-2}, with unabsorbed hard X-ray luminosities in the range $10^{42} - 10^{44}$ ergs s^{-1}. These values are typical of Compton thin Seyfert galaxies in the nearby universe. Obscured AGN with quasar-like luminosities and column densities extending to the Compton thick regime are foreseen by the synthesis models of the XRB based

on the AGN unified scheme (§ 8.3). Although it has been predicted (Fabian, Wilman, & Crawford 2002) that deep (of order a million seconds) *Chandra* exposures should detect several tens of distant, optically faint, Compton thick quasars, the observational evidence for such sources is rather scanty. Indeed, only a handful of obscured sources with quasar luminosities ($L_X > 10^{44}$ ergs s^{-1}) have been discovered so far (e.g., Stern et al. 2002), with only a marginal indication of column densities in excess of 10^{24} cm^{-2} in a few objects (Norman et al. 2002; Wilman et al. 2003). The low signal-to-noise X-ray spectrum of the high redshift ($z = 3.7$) quasar *Chandra* Deep Field-South-202 (CDF-S-202) can be equally well fitted by a transmission model with $N_H \simeq 8 \times 10^{23}$ cm^{-2} and by a reflection dominated continuum implying a heavily Compton thick source (Norman et al. 2002). In both cases, the iron line EW is of order 1 keV, though the detection is significant only at the 2σ level. The optical spectrum is dominated by narrow lines with an average FWHM of order 1500 km s^{-1} and no continuum, as expected for a type II quasar.

Detections of Compton thick sources with quasar luminosities also have been reported from X-ray observations of hyperluminous infrared galaxies (HyLIRGs). The power source responsible for an observed rest-frame $1 - 1000$ μm luminosity in excess of 10^{13} L$_\odot$ in these objects is thought to be a mixture of obscured star formation and AGN activity.

The best evidence for a deeply buried ($N_H \geq 5 \times 10^{24}$ cm^{-2}), luminous quasar ($L_{10-100 \text{ keV}} \simeq 1.7 \times 10^{46}$ ergs s^{-1}) comes from broadband *BeppoSAX* observations to ~ 100 keV of the HyLIRG IRAS 09104+4109, the most luminous object in the universe at $z < 0.5$ (Franceschini et al. 2000). Unfortunately, the *BeppoSAX* sensitivity above 10 keV does not allow other deeply buried HyLIRGs to be detected in this way. However, more sensitive *XMM-Newton* observations below $8-10$ keV provide some indirect evidence of Compton thick obscuration in two additional X-ray luminous HyLIRGs (Wilman et al. 2003).

Despite the above results that indicate that Compton thick quasars do indeed exist, the present observations suggest that their relative fraction among the obscured AGN population at high redshifts is likely to be much lower than in the nearby universe.

The disagreement between optical and X–ray classifications (already discussed in § 8.2) may be responsible for the difficulties encountered in the search for, and classification of, distant obscured sources. Indeed, one of the most surprising findings of the *Chandra* and *XMM-Newton* surveys is the discovery of a sizable number of relatively bright X-ray sources spectroscopically identified with early-type "normal" galaxies without any obvious signatures of nuclear activity in their optical spectra (Mushotzky et al. 2000; Fiore et al. 2000; Barger et al. 2001a,b;

Hornschemeier et al. 2001; Giacconi et al. 2001) It should be pointed out that the presence of relatively bright X-ray sources in the nuclei of optically dull galaxies was first recognized by *Einstein* observations (Elvis et al. 1981). The very nature of X-ray Bright Optically Normal Galaxies (hereafter, XBONG) is still a matter of debate. Multiwavelength observations of a small sample of 10 "bona fide" sources belonging to this class were discussed by Comastri et al. (2002a). The high X-ray luminosities and the relative ratios between X-ray, optical, and radio fluxes strongly suggest that nuclear activity is present in almost all the XBONG. A detailed investigation of what can be considered the prototype of this class of object (P3; Comastri et al. 2002b) indicates that a heavily obscured (possibly Compton thick) AGN is the most likely explanation. Further evidences favouring the Compton thick absorption have been presented by Comastri et al. (2003).

However, such a possibility is not unique, and alternative solutions could still be viable. For example, the broadband properties of two XBONG discussed by Brusa et al. (2003) are more consistent with those of a BL Lacertae object and a small group of galaxies, respectively. It also has been pointed out (Moran, Filippenko, & Chornock 2002; see also Moran, this volume) that optical spectroscopy sometimes can be inefficient in revealing the presence of an AGN, especially at faint fluxes, when only low quality optical spectra are in hand. The nuclear emission lines easily could be diluted by the host galaxy starlight. Indeed, AGN features in the optical band were found in three bright candidate XBONG, serendipitously discovered by *XMM-Newton* (Severgnini et al. 2003), thanks to high signal-to-noise ratio spectroscopic observations that were able to separate the nuclear spectrum from that of the host galaxy. The X-ray and optical properties could then be explained by moderately luminous ($L_X \sim 10^{42-43}$ ergs s^{-1}), mildly obscured ($N_H \sim 10^{22}$ cm^{-2}) AGN hosted by luminous galaxies. While it is almost certain that XBONG are powered by accretion onto a supermassive black hole, it remains to be proved that Compton thick absorption is ubiquitous among these sources.

High redshift Compton thick AGN could be hiding among the relatively large number of X-ray sources that have remained so far unidentified due to their extremely faint optical counterparts. The ratio between X-ray flux and optical magnitude (defined as $\log F_X/F_{opt} = \log F_X + 5.5 + R/2.5$, see Maccacaro et al. 1988; Barger et al. 2002; McHardy et al. 2003) is considered to be a fairly reliable indicator of the X-ray source classification. Indeed, the distribution of F_X/F_{opt} values of most of the spectroscopically identified X-ray selected AGN from *ROSAT* (Hasinger et al. 1998), *ASCA* (Akiyama et al. 2003), *Chandra* (Giacconi et al. 2001)
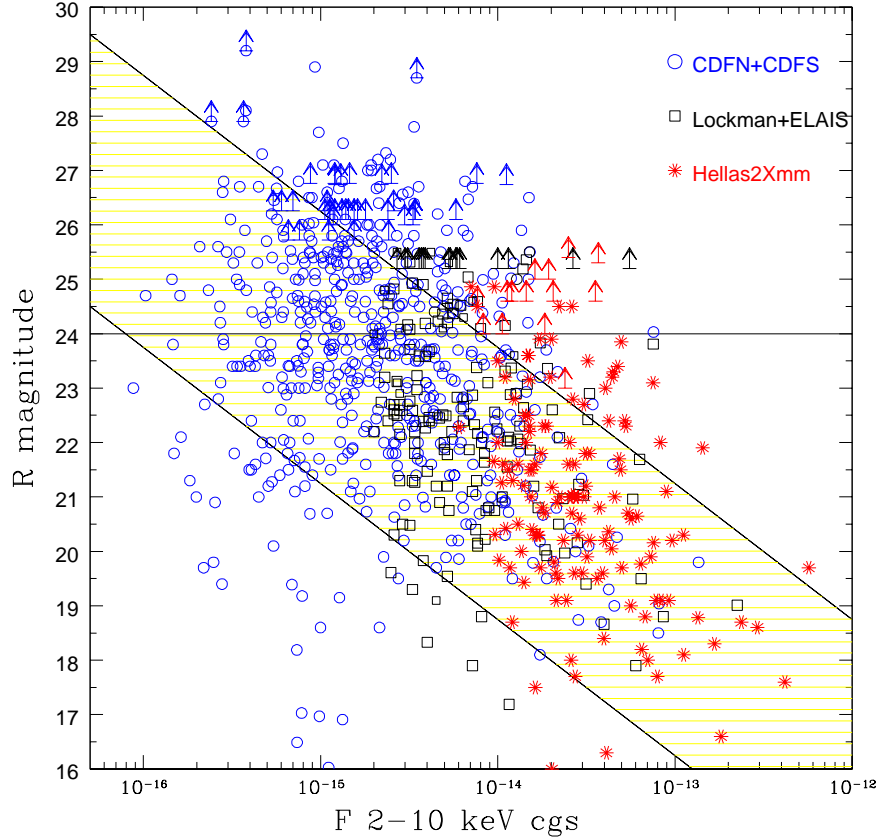
Figure 8.6. Optical R magnitude vs. $2-10$ keV flux for hard X-ray selected sources in deep *Chandra* and medium deep *XMM-Newton* surveys *(labeled)*.

and *XMM-Newton* (Mainieri et al. 2002; Fiore et al. 2003) surveys fall within $-1 < \log F_X/F_{opt} < 1$.

A sizable fraction (of order 20%) of hard X-ray selected sources are characterized by $\log F_X/F_{opt} > 1$ (Fig. 8.6). Obscured accretion seems to provide the most likely explanation for high F_X/F_{opt} values. Such a possibility was confirmed by deep VLT spectroscopy of a few X-ray bright sources that turned out to be high redshift, type II AGN (Fiore et al. 2003). It has been further suggested (Comastri et al. 2003) that high, and even extreme, values of $\log F_X/F_{opt}$ could be easily reproduced by shifting the broadband spectral energy distribution (SED), including the host galaxy starlight, of prototype Compton thick

sources (i.e., NGC 6240 and IRAS 09104+4109) over a range of redshifts ($z = 0.5 - 1.5$). This range should be considered indicative, as the optically faintest sources, especially those not detected in the R band images, could be at greater distances. The combined effect of the K-corrections on the observed optical and hard X–ray fluxes due to the very shape of the NGC 6240 SED (Fig. 8.7) is responsible for the non–linear behavior of the F_X/F_{opt} ratio as a function of redshift.
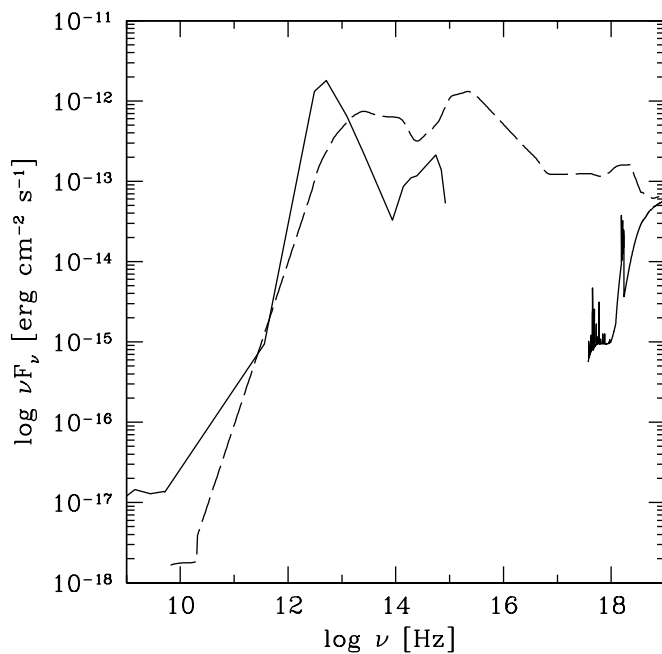

Figure 8.7. Spectral energy distribution of NGC 6240 *(continuous line)* and of the average spectrum of radio-quiet quasars (Elvis et al. 1994; *dashed line*) showing a significantly different behavior at both UV/optical and X-ray frequencies.

In order to establish whether the high values of X-ray to optical flux ratios are due to Compton thick obscuration, good quality X-ray spectra are needed to search for the characteristic absorption and reflection features of thick matter. In particular, the detection of a strong redshifted iron Kα line would provide strong evidence for Compton thick gas and, most importantly, would allow a reliable redshift measurement to be obtained for objects with optical magnitudes beyond the spectroscopic limit of large optical telescopes. Unfortunately, the X-ray count-
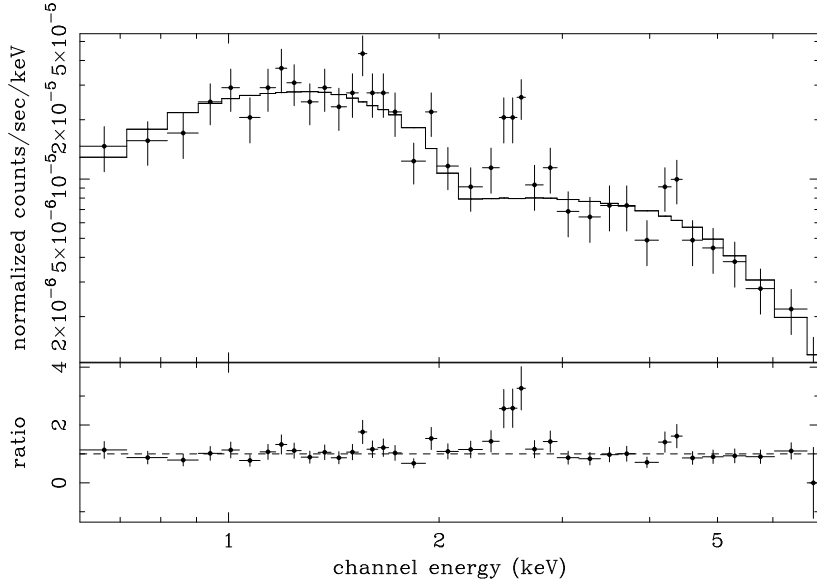
Figure 8.8. Simulated spectrum of a reflection dominated $F_{2-10 \text{ keV}} \sim 10^{-15}$ ergs cm^{-2} s^{-1} source at $z = 1.5$, as would be seen with an ultradeep 10 Ms *Chandra* observation. Input parameters are a flat power law with Γ=1 plus an iron line with an observed EW of 600 eV. The line feature is clearly seen in the residuals (bottom panel) of a single power law fit.

ing statistics, even in the deep *Chandra* fields, are not such that they can properly address this issue, possibly explaining the small fraction ($\sim 7\%$) of CDF-N sources showing iron Kα emission lines (Bauer et al. 2003).

A systematic search for strong (EW $\sim 1 - 2$ keV), redshifted iron lines among relatively faint ($F_{2-10 \text{ keV}} \sim 10^{-15}$ ergs cm^{-2} s^{-1}) hard X-ray sources would require extremely deep (of order 10 Ms) *Chandra* observations (Fig. 8.8). These are not limited, at least in the inner part of the detector, by source confusion, thanks to the good point spread function (PSF).

The fraction of X-ray sources versus intrinsic column density predicted by current synthesis models is shown in Figure 8.9. The relative number of sources with column densities larger than 10^{24} cm^{-2} starts to increase below fluxes of order 10^{-15} ergs cm^{-2} s^{-1}, reaching a fraction of order 10% of the entire X-ray source population around the limit of the deepest *Chandra* survey ($F_{2-10 \text{ keV}} \sim 2 \times 10^{-16}$ ergs cm^{-2} s^{-1}). A similar fraction is also predicted by the Ueda et al. (2003) model, which is based on quite different prescriptions for the evolution of the luminosity function.
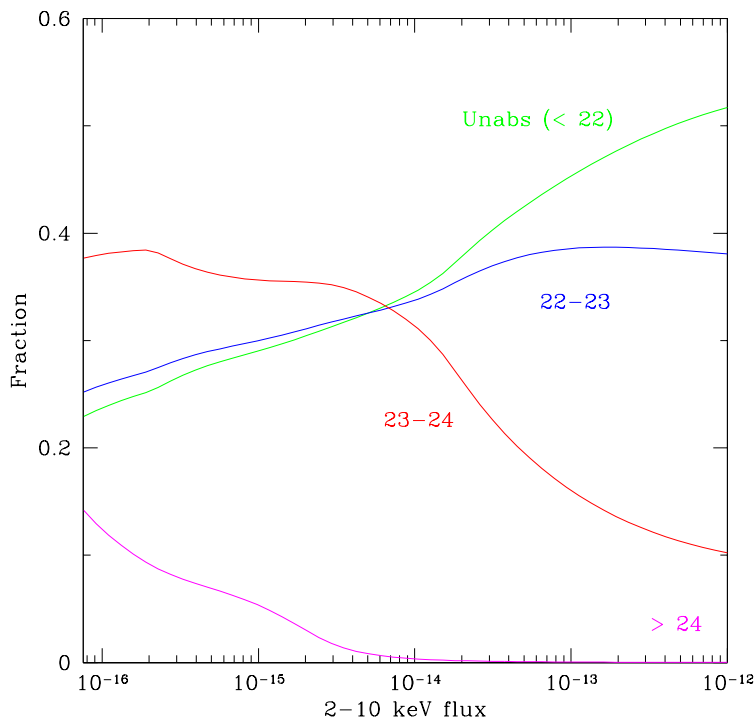
Figure 8.9. Relative fraction of sources with different column densities (labeled) vs. X-ray flux.

The small area covered with good spatial resolution by a single ACIS field would imply that at least a few pointings are needed to collect a sizable number of sources for statistical investigations. Such a project, although technically feasible, appears to be extremely challenging in terms of observing time. The search for Compton thick AGN through an X-ray selection based on the detection of a strong iron line appears to be rather inefficient and probably not worth pursuing.

8.5 Black Hole Mass Density of Compton Thick Sources

The local density in black holes grown by accretion with efficiency η can be computed using the integral argument originally proposed by Soltan (1982). An excellent review of the method, along with a detailed discussion of the most recent determinations of the black hole mass density, is presented by Fabian (2004). Here I limit myself to estimating

the black hole mass accreted during the Compton thick phase, $\rho_\bullet(CT)$, under the hypothesis that the Compton thick source contribution to the XRB is that reported in Figure 8.3.

The unabsorbed $2-10$ keV X-ray flux that enters into the computation of $\rho_\bullet(CT)$ is obtained by assuming $\Gamma=2$ and $N_H = 3 \times 10^{24}$ cm^{-2},

$$\rho_\bullet(CT) = \frac{k_{bol}}{\eta c^2} \, (1 + \langle z \rangle) \, 8.2 \times 10^{-18} \text{ ergs cm}^{-3} . \qquad (8.1)$$

The calculation of $\rho_\bullet(CT)$ then requires the knowledge of the bolometric correction term, the average redshift of the sources, and the accretion efficiency. For the latter, a standard value of $\eta = 0.1$ is assumed, while for the average redshift, the latest results of optical identifications suggest $\langle z \rangle \sim 1$ (e.g., Gilli 2004). The bolometric correction from the unabsorbed $2-10$ keV luminosity to the total luminosity is known to be a function of the X-ray luminosity. Correction factors in the range $k_{bol} \sim 10-20$ appear to be appropriate for low luminosity Seyfert-like objects (Fabian 2004), to be compared with values in the range $30-50$ for high luminosity unobscured quasars (Elvis et al. 1994). As far as the two well studied prototype Compton thick sources NGC 6240 and IRAS 09104+4109 are concerned, a direct calculation from broadband literature data, including the contribution of the host galaxy, provides remarkably similar results: $k_{bol} \sim 10$. A more precise estimate of the bolometric correction factor as a function of the X–ray properties is not possible with the present data. *Spitzer Space Telescope* observations of well defined samples of obscured AGN will provide a significant step forward in this direction.

Taking the above estimates for k_{bol}, η, and $\langle z \rangle$ at face value, the black hole mass density accreted in the Compton thick phase is about 3×10^4 M$_\odot$ Mpc^{-3}. This value could be slightly higher (up to 5×10^4 M$_\odot$ Mpc^{-3}) if the intrinsic spectral parameters are different. Based on the same argument, but following a slightly different approach, Fabian (2004) concluded that $\rho_\bullet(CT) < 10^5$ M$_\odot$ Mpc^{-3}. Unless the estimates of k_{bol}, the average redshift, and the relative contribution of Compton thick sources to the XRB are revised upwards (which seems rather unlikely), they only account for some 10% of the black hole mass density grown by accretion. Thus, most of the black hole mass density is due to less obscured Compton thin sources and unobscured quasars (see Cowie & Barger, this volume).

8.6   Contribution to the Far-IR Background

The X-ray and UV energy density absorbed by the torus of type II AGN is reemitted at longer wavelengths, most likely in the far-IR. It is thus plausible that obscured AGN may significantly contribute to

the extragalactic background light in this band. In principle, such a calculation could be performed following the guidelines discussed in § 8.3 for the synthesis of the XRB spectrum. In practice, such an approach is unfeasible, mainly because the average AGN spectral shape at long wavelengths is still rather uncertain, both from an observational and from a theoretical point of view.

In order to overcome these difficulties, a simple integral argument can been employed to compute the AGN contribution to the far-IR background. The reprocessed luminosity is estimated from the hard X-ray luminosity using the XRB intensity as an upper limit of the total energy output (Fabian & Iwasawa 1999). If one further assumes reasonable values for the effective temperature of the reprocessing dust and the cosmological evolution of the luminosity function, as determined from X-ray surveys (Almaini, Lawrence, & Boyle 1999; Brusa, Comastri, & Vignali 2001; Risaliti, Elvis, & Gilli 2002), it is also possible to estimate the spectral shape of the long wavelength background due to X-ray emitting AGN.

The different approaches come to a similar result: obscured AGN contribute from a few percent up to a maximum of $10-15\%$ at wavelengths longer than about 100μm, being possibly higher in the mid-IR ($15-60\mu$m; Risaliti et al. 2002). These findings are in relatively good agreement with observations in the infrared and submillimeter bands. The cross-correlation of *ISO* and *XMM-Newton* sources in the Lockman Hole (Fadda et al. 2002) indicates an AGN contribution of about 15-20% at 15μm (see also Alexander et al. 2002), which is similar to that estimated by Matute et al. (2002) from the optical identifications of the *ELAIS* field. In the submillimeter, Barger et al. (2001c) found that the ensemble of X-ray sources in the 1 Ms exposure of the CDF-N with SCUBA observations contribute about 15% of the extragalactic light at 850μm. According to the deepest investigation so far carried out using the 2 Ms CDF-N data (Alexander et al. 2003), many SCUBA sources are rather faint at high energies, suggesting that most of the submillimeter background is due to stellar processes.

An attempt to estimate the contribution of Compton thick sources to the long wavelength background is discussed by Brusa et al. (2001). Assuming the XRB model of Comastri et al. (1995) and the observed correlations between the hard X-ray and far-IR luminosities of bright nearby AGN as a function of the absorbing column density, these authors concluded that, although not energetically dominant, the most important contribution to the far-IR background comes from Compton thick sources (Fig. 8.10).

If anything, heavily obscured Compton thick sources appear to be the most favored class of AGN to be detected in the far-IR/submillimeter bands. The issue of the nature of the far-IR background will greatly benefit from upcoming *Spitzer Space Telescope* observations.
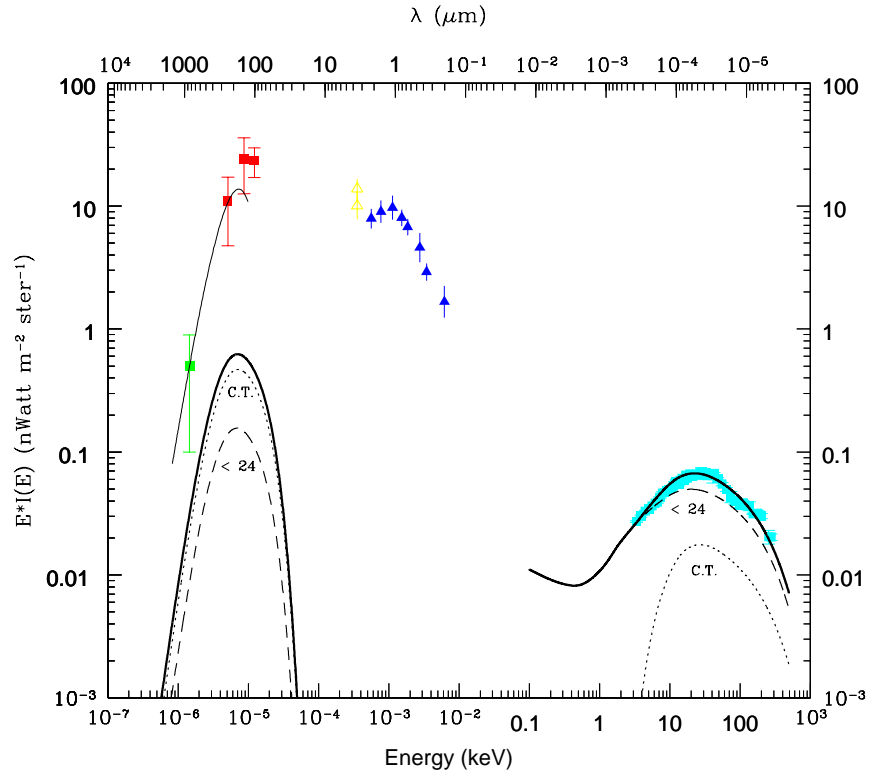

Figure 8.10. Model predicted AGN contribution at far-IR and X-ray wavelengths (solid thick line). Dashed line represents contribution of Compton thin sources, while dotted line that of Compton thick sources. Data points are from a compilation of measurements of the extragalactic background intensity from Fixsen et al. (1998; submillimeter data and best fit curve—thin black curve), Lagache et al. (2000; far-IR data), Dwek & Arendt (1998; DIRBE mid-IR data), Pozzetti et al. (1998; optical and near-IR data) and Marshall et al. (1980; X-ray data).

8.7   Conclusions and future prospects

Different sets of X-ray observations and theoretical arguments indicate that the reprocessing of high energy radiation by Compton thick matter in the circumnuclear regions of AGN is very common, if not ubiquitous. Unfortunately, even the most sensitive hard X-ray surveys

carried out with the *Chandra* and *XMM-Newton* observatories turn out to be rather inefficient for searching for the typical signatures of thick matter. Further observations, though useful in several respects, will not provide the breakthrough in this direction. In fact, according to what can be considered a solid model for the XRB, only a small fraction of the Compton thick population could be detected by present X-ray surveys below $8-10$ keV.

A mission capable of exploring the hard X-ray sky in the $10-70$ keV band with focusing/imaging instruments able to reach fluxes of order 10^{-14} ergs cm^{-2} s^{-1} would provide a quantum leap forward. As an order of magnitude estimate, the three dex jump in the limiting flux would be similar to that achieved by *BeppoSAX* and *ASCA* in the $2-10$ keV band with respect to the *HEAO1-A2* survey of Piccinotti et al. (1982). In other words, such a gain in sensitivity would push the resolved fraction of the hard ($10-70$ keV) XRB from a negligible 1% to about $30-40\%$. Sensitive, high energy surveys will open up a large volume of discovery space that so far only has been touched by *BeppoSAX* observations. It is important to stress that the scientific output of these observations would be even more rewarding than a mere improvement in the limiting flux, as the $10-70$ keV band fully encompasses the peak of the XRB energy density at 30 keV.

The X-ray Evolving Universe Spectrometer *(XEUS)* mission, currently under study to be the next ESA cornerstone mission for X-ray astronomy, will be capable of surveying the hard X-ray sky at, or even below, 10^{-14} ergs cm^{-2} s^{-1} to energies of $40-50$ keV. Obviously, the scientific objectives of such a mission would be much broader than a better sampling of the Compton thick population. The mission would be devoted to probing a significant fraction of the electromagnetic radiation from accretion onto supermassive black holes.

Acknowledgments

References

Akiyama, M., Ueda, Y., Ohta, K., Takahashi, T., & Yamada T. 2003, ApJS, 148, 275

Akiyama, M., et al. 2000, ApJ, 532, 700

Alexander, D. M., et al. 2002, ApJ, 568, L85

Alexander, D. M., et al. 2003, AJ, 126, 539

Almaini, O., Lawrence, A., & Boyle, B. J. 1999, MNRAS, 305, L59

Antonucci, R. R. J. 1993, ARA&A, 31, 473

Barger, A. J., Cowie, L. L., Bautz, M. W., Brandt, W. N., Garmire, G. P., Hornschemeier, A. E., Ivison, R. J., & Owen, F. N. 2001a, AJ, 122, 2177

Barger, A. J., Cowie, L. L., Brandt, W. N., Capak, P., Garmire, G. P., Hornschemeier, A. E., Steffen, A. T., & Wehner, E. H. 2002, AJ, 124, 1839

Barger A. J., Cowie L. L., Mushotzky R.F., & Richards E.A. 2001b, AJ 121, 662

Barger, A. J., Cowie, L. L., Steffen, A. T., Hornschemeier, A. E., Brandt, W. N., & Garmire, G. P. 2001c, ApJ, 560, L23

Barger, A. J., et al. 2003, AJ, 126, 632

Bassani, L., Dadina, M., Maiolino, R., Salvati, M., Risaliti, G., della Ceca, R., Matt, G., & Zamorani, G. 1999, ApJS, 121, 473

Bauer, F. E., et al. 2003, AN, 324, 175

Braito, V., et al. 2003, A&A, 398, 107

Brusa, M. 2004, PhD thesis, Bologna University

Brusa, M., Comastri, A., & Vignali, C. 2001, in "Clusters of Galaxies and the High Redshift Universe Observed in X-rays", Eds. D. M. Neumann, & J. T. T. Van (astro-ph/0106014)

Brusa, M., et al. 2003, A&A, 409, 65

Cappi, M., et al. 1999, A&A, 344, 857

Collinge, M. J., & Brandt, W. N. 2000, MNRAS, 317, L35

Comastri, A. 1991, PhD thesis, Bologna University

Comastri, A., Setti, G., Zamorani, G., & Hasinger, G. 1995, A&A, 296, 1

Comastri, A. 2001, in "X-ray Astronomy: Stellar Endpoints, AGN, and the Diffuse X-ray Background", Eds. N. E. White, G. Malaguti, & G. G. C. Palumbo. (Melville, New York: AIP Conference Proceedings), 599, p73

Comastri, A., Fiore, F., Vignali, C., Matt G., Perola, G.C., La Franca, F. 2001, MNRAS, 327, 781

Comastri, A., et al. 2002a, in "New Visions of the X-ray Universe in the XMM-*Newton* and *Chandra* Era", Ed. F. Jansen. (Noordwijk: ESA/ESTEC), ESA SP-488 (astro-ph/0203019)

Comastri, A., et al. 2002b, ApJ, 571, 771

Comastri, A., et al. 2003, AN, 324, 28

Della Ceca, R., et al. 2002, ApJ, 581, L9

Dwek, E., & Arendt, R. G. 1998, ApJ, 508, 9

Elvis, M., Schreier, E.J., Tonry, J., Davis, M., Huchra, J. P. 1981, ApJ, 246, 20

Elvis, M., et al. 1994, ApJS, 95, 1

Fabian, A. C. 2004, in "Coevolution of Black Holes and Galaxies", Carnegie Observatories Astrophysics Series, Vol. 1, Ed. L. C. Ho. (Cambridge, U.K.: Cambridge University Press), in press (astro-ph/0304122)

Fabian, A. C., George, I. M., Miyoshi, S., & Rees, M. J. 1990, MNRAS, 242, 14

Fabian, A. C., & Iwasawa, K. 1999, MNRAS, 303, L34

Fabian, A. C., Wilman, R. J., & Crawford, C. S. 2002, MNRAS, 329, L18

Fadda, D., et al. 2002, A&A, 383, 838

Fiore, F., et al. 2000, NewA, 5, 143

Fiore, F., et al. 2003, A&A, 409, 79

Fixsen, D. J., Dwek, E., Mather, J. C., Bennett, C. L., & Shafer, R. A. 1998, ApJ, 508, 123

Franceschini, A., Bassani, L., Cappi, M., Granato, G. L., Malaguti, G., Palazzi, E., & Persic, M. 2000, A&A, 353, 910

Fukazawa, Y., Iyomoto, N., Kubota, A., Matsumoto, Y., & Makishima, K. 2001, A&A, 374, 73

George, I. M., & Fabian, A. C. 1991, MNRAS, 249, 352

Ghisellini, G., Haardt, F., & Matt, G. 1994, MNRAS, 267, 743

Giacconi, R., et al. 2001, ApJ, 551, 664

Giacconi, R., et al. 2002, ApJS, 139, 639

Gilli, R. 2004, in "New Results from Clusters of Galaxies and Black Holes", Advances in Space Research, Eds. C. Done, E. M. Puchnarewicz, & M. J. Ward. (Amsterdam: Elsevier Science), in press (astro-ph/0303115)

Gilli, R., Salvati M., & Hasinger G., 2001, A&A, 366, 407

Guainazzi, G., Matt, G., Brandt, W. N., Antonelli, L. A., Barr, P., & Bassani, L. 2000, A&A, 356, 463

Guainazzi, M., Matt, G., Perola, G.C., & Fiore F. 2002, in "Workshop on X-ray spectroscopy of AGN with Chandra and XMM-Newton". MPE report 279, p203

Guainazzi, M., Stanghellini, C., & Grandi, P. 2003, in "XEUS–Studying the Evolution of the Hot Universe", Eds. G. Hasinger, Th. Boller, & A. N. Parmer. MPE Report 281, p261

Guainazzi, M., et al. 1999, MNRAS, 310, 10

Hasinger, G., Burg, R., Giacconi, R., Schmidt, M., Trumper, J., & Zamorani, G. 1998, A&A, 329, 482

Hasinger, G., et al. 2001, A&A, 365, L45

Hornschemeier, A. E., et al. 2001, ApJ, 554, 742

Iwasawa, K., & Comastri, A. 1998, MNRAS, 297, 1219

Iwasawa, K., Matt, G., Fabian, A. C., Bianchi, S., Brandt, W. N., Guainazzi, M., Murayama, T., & Taniguchi, Y. 2001, MNRAS, 326, 119

Iwasawa, K., Maloney, P. R., & Fabian, A.C. 2002, MNRAS, 336, L71

Iyomoto, N., Fukazawa, Y., Nakai, N., & Ishihara, Y. 2001, ApJ, 561, L69

Kleinmann, S. G., Hamilton, D., Keel, W. C., Wynn-Williams, C. G., Eales, S. A., Becklin, E. E., & Kuntz, K.D 1988, ApJ, 328, 161

Lagache, G., Haffner, L. M., Reynolds, R. J., & Tufte, S. L. 2000, A&A, 354, 247

Leahy, D. A., & Creighton, J. 1993, MNRAS, 263, 314

Levenson, N. A., Krolik, J. H., Zycki, P. T., Heckman, T. M., Weaver, K. A., Awaki, H., & Terashima, Y. 2002, ApJ, 573, L81

Levenson, N. A., Weaver, K. A., Heckman, T. M., Awaki, H., & Terashima, Y., 2004, ApJ, 602, 135

Maccacaro, T., Gioia, I. M., Wolter, A., Zamorani, G., & Stocke, J. T. 1988, ApJ, 326, 680

Madau, P., Ghisellini, G., & Fabian, A. C. 1994, MNRAS, 270, 17

Mainieri, V., et al. 2002, A&A, 393, 425

Maiolino, R., et al. 1998, A&A, 338, 781

Maiolino, R., et al. 2003, MNRAS, 344, L59

Malaguti, G., et al. 1998, A&A, 331, 519

Marshall, F. E., et al. 1980, ApJ, 235, 4

Matt, G. 2000, A&A, 355, L31

Matt, G. 2002, RSPTA, 360, 2045

Matt, G., Brandt, W. N., & Fabian, A. C. 1996, MNRAS, 280, 823

Matt, G., Fabian, A. C., Guainazzi, M., Iwasawa, K., Bassani, L., & Malaguti, G. 2000, MNRAS, 318, 173

Matt, G., Guainazzi, M., & Maiolino, R. 2003, MNRAS, 342, 422

Matt, G., Perola, G. C., & Piro L. 1991, A&A 247, 25

Matt, G., et al. 1996, MNRAS, 281, L69

Matt, G., et al. 1997, A&A, 325, L13

Matt, G., et al. 1999, A&A, 341, L39

Matute I., et al. 2002, MNRAS, 332, L11

McHardy, I. M., et al. 2003, MNRAS, 342, 802

Moran, E. C., Filippenko, A. V., & Chornock R. 2002, ApJ, 579, L71

Murayama, T., Taniguchi, Y., & Iwasawa, K. 1998, AJ, 115, 460

Mushotzky, R. F., Cowie, L. L., Barger, A. J., & Arnaud, K. A. 2000, Nature, 404, 459

Norman, C., et al. 2002, ApJ, 571, 218

Piccinotti, G., Mushotzky, R. F., Boldt, E. A., Holt, S. S., Marshall, F. E., Serlemitsos, P. J., & Shafer, R. A. 1982, ApJ, 253, 485

Piconcelli, E., et al. 2002, A&A, 394, 835

Pozzetti, L., Madau, P., Zamorani, G., Ferguson, H. C., & Bruzual, G. 1998, MNRAS, 298, 1133

Ptak, A., Heckman, T., Levenson, N. A., Weaver, K., & Strickland, D. 2003, ApJ, 592, 782

Risaliti, G., Elvis, M., & Gilli, R. 2002, ApJ, 566, L67

Risaliti, G., Gilli, R., Maiolino, R., & Salvati, M. 2000, A&A, 357, 13

Risaliti, G., Maiolino, R., & Salvati, M. 1999a, ApJ, 522, 157

Risaliti, G., Woltjer, L., & Salvati, M. 2003, A&A, 401, 895

Risaliti, G., et al. 1999b, MmSAI, 70, 73

Schurch, N. J., Roberts, T. P., & Warwick, R. S. 2002, MNRAS, 335, 241

Setti, G., & Woltjer, L. 1989, A&A, 224, L21

Severgnini, P., et al. 2003, A&A, 406, 483

Stern, D., et al. 2002, ApJ, 568, 71

Szokoly, Y., et al. 2004, ApJS, submitted (astro-ph/0312324)

Terasawa, N. 1991, ApJ, 378, L11

Turner, T. J., George, I. M., Nandra, K., & Mushotzky, R. F. 1997, ApJ, 488, 164

Ueda, Y., Akiyama, M., Ohta, K., & Miyaji, T. 2004, ApJ, 598, 886

Ueno, S., Ward, M. J., O'Brien, P. T., Stirpe, G. M., & Matt, G. 1998, in "The Active X-ray Sky: Results from *BeppoSAX* and *RXTE*", Eds. L. Scarsi, H. Bradt, P. Giommi, & F. Fiore. Nuclear Physics B Proceedings Supplements, (Amsterdam: Elsevier Science), 69, 554

Vignali, C., & Comastri, A. 2002, A&A, 381, 834

Vignati, P., et al. 1999, A&A, 349, L57

Wilman, R. J., & Fabian, A. C. 1999, MNRAS, 309, 862

Wilman, R. J., Fabian, A. C., Crawford, C. S., & Cutri, R. M. 2003, MNRAS, 338, L19